Mechanisms of hepatic steatosis in mice fed a lipogenic methionine choline-deficient diet

Mary E. Rinella,[1,*] Marc S. Elias,[*] Robin R. Smolak,[*] Tao Fu,[*,†] Jayme Borensztajn,[†] and Richard M. Green[*]

Departments of Medicine* and Pathology,† Northwestern University Feinberg School of Medicine, Chicago, IL

Abstract The methionine choline-deficient (MCD) diet results in liver injury similar to human nonalcoholic steatohepatitis (NASH). The aims of this study were to define mechanisms of MCD-induced steatosis in insulin-resistant db/db and insulin-sensitive db/m mice. MCD-fed db/db mice developed more hepatic steatosis and retained more insulin resistance than MCD-fed db/m mice. Both subcutaneous and gonadal fat were reduced by MCD feeding: gonadal fat decreased by 23% in db/db mice and by 90% in db/m mice. Weight loss was attenuated in the db/db mice, being only 13% compared with 35% in MCD-fed db/db and db/m mice, respectively. Both strains had upregulation of hepatic fatty acid transport proteins as well as increased hepatic uptake of [^{14}C]oleic acid: 3-fold in db/m mice ($P < 0.001$) and 2-fold in db/db mice ($P < 0.01$) after 4 weeks of MCD feeding. In both murine strains, the MCD diet reduced triglyceride secretion and downregulated genes involved in triglyceride synthesis. Therefore, increased fatty acid uptake and decreased VLDL secretion represent two important mechanisms by which the MCD diet promotes intrahepatic lipid accumulation in this model. Feeding the MCD diet to diabetic rodents broadens the applicability of this model for the study of human NASH.—Rinella, M. E., M. S. Elias, R. R. Smolak, T. Fu, J. Borensztajn, and R. M. Green. **Mechanisms of hepatic steatosis in mice fed a lipogenic methionine choline-deficient diet. *J. Lipid Res.* 2008.** 49: **1068–1076.**

Supplementary key words nonalcoholic steatohepatitis • db/db mouse • lipid metabolism • visceral fat

Nonalcoholic fatty liver disease (NAFLD) is the most common cause of abnormal liver chemistry tests in the developed world and a major public health problem. Its progressive form, termed nonalcoholic steatohepatitis (NASH) (1), is a significant predisposing factor for the development of cryptogenic cirrhosis and hepatic failure and an increasingly common indication for liver transplantation (2, 3). Insulin resistance is a very significant contributor to the development of NASH that is then exacerbated by hepatic steatosis (4–6). Furthermore, strong evidence exists demonstrating that in NAFLD patients, insulin does not suppress adipose tissue lipolysis to the same extent that it does in healthy individuals (5). Human data have shown that most hepatic triglyceride in patients with NASH originates from increased delivery and subsequent uptake of free fatty acids to the liver (7).

NASH is closely associated with obesity and the metabolic syndrome; thus, obese, diabetic murine models such as leptin-deficient ob/ob mice have been used to study experimental steatohepatitis. Despite the presence of profound fatty liver, obesity, and diabetes, ob/ob mice do not develop significant liver injury because of the essential role of leptin in hepatic injury and fibrosis (8, 9). In contrast to ob/ob mice, leptin-resistant db/db mice are hyperinsulinemic, hyperleptinemic, and hyperlipidemic. They retain some leptin signaling, likely through the short-form leptin receptor, and develop hepatic fibrosis when fed a methionine choline-deficient (MCD) diet (10, 11). Feeding mice a MCD diet is a frequently used nutritional model of NASH that induces aminotransferase elevation and hepatic histological changes characterized by steatosis, focal inflammation, hepatocyte necrosis, and fibrosis (12–14). These histological changes occur rapidly and are morphologically similar to those observed in human NASH. db/db mice fed the MCD diet have greater hepatic injury, steatohepatitis, and hepatic fibrosis than db/m mice fed the MCD diet. In addition, they develop a more proinflammatory cytokine profile than db/m mice fed the MCD diet or db/db mice on a control diet (11, 14).

The mechanisms responsible for the development of hepatic steatosis in the MCD dietary model have not been fully delineated; however, previous rat studies using

Manuscript received 17 January 2007 and in revised form 23 January 2008.

Published, JLR Papers in Press, January 28, 2008.
DOI 10.1194/jlr.M800042-JLR200

Abbreviations: AOX, acyl-coenzyme A oxidase; apoB, apolipoprotein B; CPT, carnitine palmitoyltransferase; FATP, fatty acid transport protein; FPLC, fast-protein liquid chromatography; MCD, methionine choline-deficient; NAFLD, nonalcoholic fatty liver disease; NASH, nonalcoholic steatohepatitis; PPAR, peroxisome proliferator-activated receptor; QUICKI, Quantitative Insulin Sensitivity Check Index; RT, real-time; SCD-1, stearoyl-coenzyme A desaturase-1; SREBP, sterol-regulatory element binding protein.

[1] To whom correspondence should be addressed.
e-mail: m-rinella@northwestern.edu

a choline-deficient (methionine-containing) diet suggest that the pathogenesis of hepatic steatosis may be attributable, at least in part, to impaired hepatic VLDL secretion (15). This assumption is further supported by the fact that methionine and choline are precursors to phosphatidylcholine, the main phospholipid coating VLDL particles (16). In wild-type mice, others have found that the MCD diet results in downregulation of stearoyl-coenzyme A desaturase-1 (SCD-1), a key enzyme in triglyceride synthesis, with minimal upregulation of β-oxidation genes (17). Thus, impaired VLDL secretion may play a role in MCD diet-induced intrahepatic lipid accumulation in mice.

The aims of this study were to examine the effect of the MCD diet within the physiologic milieu of the metabolic syndrome that occurs in diabetic db/db mice. Furthermore, we examined the mechanisms by which the MCD diet promotes hepatic steatosis in both insulin-sensitive db/m mice and insulin-resistant db/db mice. Our data demonstrate that db/db mice fed the MCD diet retain many aspects of the metabolic syndrome and have relatively preserved visceral fat stores compared with db/m mice. Increased hepatic fatty acid uptake and reduced VLDL secretion are two important mechanisms by which the MCD diet promotes hepatic steatosis.

MATERIALS AND METHODS

Animals and diet

Female BKS·Cg-m$^{+/+}$ Lepr^{db}/J (db/db) mice and insulin-sensitive heterozygote db/m mice, 8–10 weeks of age, were obtained from the Jackson Laboratory (Bar Harbor, ME). All mice received humane care in compliance with institutional guidelines. Animals had free access to chow and water until the first day of the study, when they received their corresponding diet. The mice were fed one of two diets: a lipogenic diet deficient in methionine and choline (MCD diet) or the MCD diet supplemented with methionine and choline (control diet) (ICN Biomedicals, Inc., Costa Mesa, CA) for 4 weeks. After a 4 h fast, animals were euthanized using CO_2 narcosis. Whole blood was obtained from the right atrium by cardiac puncture, and the livers were excised and weighed. Livers were flash-frozen in liquid nitrogen and stored at −70°C. All animal experiments were approved by the Animal Care and Use Committee of Northwestern University Feinberg School of Medicine.

Biochemical analysis

The determination of serum alanine aminotransferase was performed using a spectrophotometric assay kit (Biotron, Hemet, CA), and values are reported in Sigma-Frankel units/ml. Triglyceride (TG) and cholesterol were measured enzymatically (Thermo Electron, Louisville, KY) on serum and hepatic homogenate. Fasting blood glucose was measured by the glucose oxidase method using a reflectance glucometer (One Touch II; LifeScan, Milpitas, CA), and serum insulin and leptin levels were determined via radioimmunoassay (Linco, St. Charles, MO). Quantitative Insulin Sensitivity Check Index (QUICKI) was calculated from fasting insulin and glucose levels. Serum β-hydroxybutyrate levels were determined using the β-hydroxybutyrate Liquicolor method (Sanbio, Boerne, TX).

Measurement of visceral (gonadal) and subcutaneous adipose tissue compartments

After CO_2 narcosis and removal of the liver, representative depots of both gonadal (parametrial and paraovarian), representative of visceral fat, and subcutaneous adipose tissue were obtained from all mice in each group as described previously (18). Subcutaneous fat was removed in a standardized manner from the skin overlying the abdominal wall bordered inferiorly by the perineum, medially by the abdominal midline (defined by the most medial aspect of the rectus abdominus), laterally by the midaxillary line, superiorly by the xyphoid process, and posteriorly by the spine.

Measurement of VLDL secretion

Four cohorts of five mice each were fasted overnight, anesthetized with 70 mg/kg ketamine and 7 mg/kg xylazine ip, and then injected with 0.2 ml of a 10% (v/v) solution of Triton WR-1339 in saline. Blood samples were collected from the tail vein at 0, 3, and 6 h. During the entire period, the animals had free access to water. Triglyceride and cholesterol assays were performed as described above. Assuming that total blood volume in the mouse represents 3.5% of its body weight (19), the rate of triglyceride accumulation in mg/kg/h was determined after inhibitor (Triton WR-1339) injection. Plasma apolipoprotein B-100 (apoB-100) and apoB-48 were detected using Western immunoblotting. Aliquots of the plasma before and after Triton WR-1339 injection were diluted 1:2 (v/v) with denaturing sample buffer, heated at 70°C for 10 min, and run on a 3–8% Tris acetate gel using the NuPAGE electrophoresis system (Invitrogen, Carlsbad, CA). The aliquots were then transferred to a nitrocellulose membrane using the wet electrophoretic transfer. Immunoblotting was performed on a nitrocellulose membrane with rabbit polyclonal antibodies (Biodesign International, Saco, ME) against mouse apoB-48/apoB-100 as described previously (20).

Fast-protein liquid chromatography

Serum lipoproteins were fractionated with an ÄKTA fast-protein liquid chromatography (FPLC) system using equal volumes of pooled plasma from mouse cohorts on tandem Superose 6 FPLC columns (Amersham Biosciences, Piscataway, NJ). The columns were then eluted with 200 mmol/l sodium phosphate (pH 7.4), 50 mmol/l NaCl, 0.03% (w/v) EDTA, and 0.02% (w/v) sodium azide at a flow rate of 0.4 ml/min. The contents of TG and cholesterol in the eluted fractions and plasma were measured with a microplate assay technique using enzymatic assay reagent kits (Sigma, St. Louis, MO).

Hepatic [^{14}C]oleic acid uptake

Hepatic [^{14}C]oleate uptake was measured as described previously by Doege et al. (21). Briefly, in a separate experiment, four cohorts of five female db/m and db/db mice were treated for 4 weeks on their respective diets and then fasted overnight with free access to water. Each mouse then received an intragastric 200 μl olive oil bolus containing 2 μCi of [^{14}C]oleic acid (0.1 mCi/ml; ARC 0297-50μCi; American Radiolabeled Chemicals, Inc., St. Louis, MO). Because the exact oleic acid content of the olive oil was unknown, results were analyzed as relative uptake in disintegrations per minute in the four groups rather than as absolute uptake. Before (time 0) and at 30, 60, 120, and 240 min after administration, blood samples were collected via tail bleed. The liver was resected at the 240 min time point, and 250 mg of liver was homogenized in 1 ml of Dulbecco's phosphate-buffered saline.

TABLE 1. Primer sequences for real-time quantitative PCR

Primer	Sequence
AOX-fwd	5′-CTT GTT CGC GCA AGT GAG G-3′
AOX-rev	5′-CAG GAT CCG ACT GTT TAC C-3′
CPT2-fwd	5′-GCC CAG CTT CCA TCT TTA CT-3′
CPT2-rev	5′-CAG GAT GTT GTG GTT TAT CCG C-3′
FAS-fwd	5′-TGC TCC CAG CTG CAG GC-3′
FAS-rev	5′-GCC CGG TAG CTC TGG GTG TA-3′
FATP1-fwd	5′-CGC TTT CTG CGT ATC GTC TG-3′
FATP1-rev	5′-GAT GCA CGG GAT CGT GTC T-3′
FATP2-fwd	5′-GGT ATG GGA CAG GCC TTG CT-3′
FATP2-rev	5′-GGG CAT TGT GGT ATA GAT GAC ATC-3′
FATP3-fwd	5′-AGT GCC AGG GAT TCT ACC ATC-3′
FATP3-rev	5′-GAA CTT GGG TTT CAG CAC CAC-3′
FATP4-fwd	5′-GAT GGC CTC AGC TAT CTG TGA-3′
FATP4-rev	5′-GGT GCC CGA TGT GTA GAT GTA-3′
FATP5-fwd	5′-CTA CGC TGG CTG CAT ATA GAT G-3′
FATP5-rev	5′-CCA CAA AGG TCT CTG GAG GAT-3′
GAPDH-fwd (1)	5′-ACC ACC ATG GAG AAG GCC GG-3′
GAPDH-rev (1)	5′-CTC AGT GTA GCC CAA GAT GC-3′
GAPDH-fwd (2)	5′-GTC GTG GAT CTG ACG TGC C-3′
GAPDH-rev (2)	5′-TGC CTG CTT CAC CAC CTT C-3′
LCAD-fwd	5′-AAG GAT TTA TTA AGG GCA AGA AGC-3′
LCAD-rev	5′-GGA AGC GGA GGC GGA GTC-3′
L-FABP-fwd	5′-GTG GTC CGC AAT GAG TTC AC-3′
L-FABP-rev	5′-GTA TTG GTG ATT GTG TCT CC-3′
SCD-1-fwd	5′-TGG GTT GGC TGC TTG TG-3′
SCD-1-rev	5′-GCG TGG GCA GGA TGA AG-3′
SREBP-1a-fwd	5′-TAG TCC GAA GCC GGG TGG GCG CCG GCG CCA T-3′
SREBP-1a-rev	5′-GAT GTC GTT CAA AAC CGC TGT GTG TCC AGT TC-3′
SREBP-1C-fwd	5′-ATC GGC GCG GAA GCT GTC GGG GTA GCG TC-3′
SREBP-1C-rev	5′-ACT GTC TTG GTT GTT GAT GAG CTG GAG CAT-3′

AOX, acyl-coenzyme A oxidase; CPT, carnitine palmitoyltransferase; FATP, fatty acid transport protein; LCAD, long-chain acyl-coenzyme A dehydrogenase; L-FABP, fatty acid binding protein; SCD-1, stearoyl-coenzyme A desaturase-1; SREBP, sterol-regulatory element binding protein.

Liver homogenate (0.8 ml) was added to a mixture of 1 ml of chloroform and 2 ml of methanol. The sample was vortexed for 1 min, and 1 ml of Millipore water and an additional 1 ml of chloroform were then added. The sample was vortexed again and then spun at 2,000 rpm for 5 min. The resultant lipid phase was dried, and 5 ml of ScintiVerse (Fisher Scientific, Hampton, NH) was added, in small scintillation vials, vortexed, and then counted for 2 min in a Beckman LS6500 scintillation counter whose efficiency was calculated to be 95%.

RNA extraction and quantitative real-time PCR

Total RNA was extracted from liver by homogenizing snap-frozen liver tissue samples in TRIzol reagent (Invitrogen). cDNA was synthesized from 2 μg of total RNA using the SuperScript First Strand System for real-time (RT)-PCR (Invitrogen) and random hexamer primers. The resulting cDNA was subsequently used as a template for quantitative RT-PCR. RT-PCR was performed using 4 μl of the total cDNA in a 50 μl reaction containing QuantiTect SYBR Green PCR Master Mix (Qiagen, Valencia, CA) with specific RT-PCR primers (**Table 1**). GAPDH (Integrated DNA Technologies, Coralville, IA) was used as a control. RT-PCR was performed using the Applied Biosystems Prism 5700 Sequence Detection System (Applied Biosystems, Foster City, CA). Results are reported as relative differences in gene expression.

Statistics

ANOVA was used for multiple group comparisons. When ANOVA resulted in a nonparametric distribution of the data, a log transformation was performed. When two groups were compared, unpaired *t*-tests were used for data analysis.

RESULTS

The MCD diet has been shown previously to alter glucose metabolism in other mouse strains (12). Thus, we compared the effects of the MCD diet on these metabolic parameters in db/m and db/db mice. **Table 2** summarizes the metabolic effects of the MCD diet on db/db and db/m mice. db/db mice fed either the control diet or the MCD diet remained hyperinsulinemic relative to db/m mice fed either diet (3.7 ± 0.8 and 1.6 ± 0.5 ng/ml, compared with 0.6 ± 0.1 and 0.7 ± 0.2 ng/ml, in db/m mice fed the control or MCD diet, respectively; $P < 0.05$). Similarly, db/db mice remained more insulin-resistant (lower QUICKI values) than db/m mice fed either diet. MCD-fed db/db mice had a QUICKI of 0.44 ± 0.01, compared with 0.63 ± 0.05 in db/m mice fed the MCD diet ($P < 0.05$). db/db mice remained hyperleptinemic on the MCD diet relative

TABLE 2. Metabolic parameters of fasting db/db and db/m mice fed the MCD or control diet for 4 weeks

	db/db Mice		db/m Mice	
Parameter	Control Diet	MCD Diet	Control Diet	MCD Diet
Insulin (ng/ml)	3.7 ± 0.8[a]	1.6 ± 0.5[b]	0.6 ± 0.1	0.7 ± 0.2
Glucose (mg/dl)	426 ± 74	124 ± 16	195 ± 24	76 ± 8
Quantitative Insulin Sensitivity Check Index	0.32 ± 0.02[a]	0.44 ± 0.01[b]	0.52 ± 0.03	0.63 ± 0.05
Leptin (ng/ml)	123 ± 40[a]	133 ± 23[b]	21 ± 3	19 ± 2
Alanine aminotransferase (SFU/ml)	107 ± 7[a,c]	383 ± 18[b]	29 ± 10[d]	101 ± 3
Liver triglyceride (mg/g liver)	65 ± 12[a,c]	106 ± 5	22 ± 3[d]	89 ± 13
Serum triglyceride (mg/dl)	79 ± 3[c]	56 ± 3	70 ± 4[d]	45 ± 5
Serum cholesterol (mg/dl)	216 ± 7[a,c]	148 ± 11[b]	97 ± 3[d]	69 ± 5

MCD, methionine choline-deficient; SFU, sigma-Frankel units. Data were analyzed using ANOVA (n = 4–7 for each group). Values represent means ± SEM. For all, $P < 0.05$.

[a] db/db versus db/m mice on the control diet.

[b] db/db versus db/m mice on the MCD diet.

[c] db/db mice on the control versus the MCD diet.

[d] db/m mice on the control versus the MCD diet.

TABLE 3. Body weight and food consumption after 4 weeks of feeding with the MCD or the MCD control diet

Parameter	db/db Mice		db/m Mice	
	Control Diet	MCD Diet	Control Diet	MCD Diet
Liver weight (g)	2.78 ± 0.13[a,c]	1.80 ± 0.22[b]	1.00 ± 0.07[d]	0.74 ± 0.03
Baseline body weight (g)	35.2 ± 1.5[a]	39.5 ± 2.4[b]	19.6 ± 0.3	21.7 ± 0.4
Final body weight (g)	49.8 ± 1.1[a]	34.6 ± 2.2[b]	21.3 ± 0.5	14.2 ± 0.3
Change in body weight (g) (%)	14.5 ± 0.6 (42%)[a,c]	−4.9 ± 0.6 (−13%)[b]	1.8 ± 0.5 (9%)[d]	−7.5 ± 0.2 (−35%)
Daily food consumption (g)	6.1 ± 0.4[a,c]	3.4 ± 0.5	2.9 ± 0.6	3.5 ± 1.3

Data were analyzed using ANOVA (n = 5 for each group). Values represent means ± SEM. For all, $P < 0.001$.
[a] db/db mice versus db/m mice on the control diet.
[b] db/db mice versus db/m mice on the MCD diet.
[c] db/db mice on the control versus the MCD diet.
[d] db/m mice on the control versus the MCD diet.

to db/m mice fed either diet: 133 ± 23 ng/ml compared with 19 ± 2 and 21 ± 3 ng/ml in db/m mice fed the MCD and control diet, respectively ($P < 0.001$). Table 2 also demonstrates that db/db mice fed the MCD diet had significantly higher serum cholesterol levels than db/m mice fed either diet. In addition, there was an upward trend in serum triglyceride levels for db/db mice fed the MCD diet compared with db/m mice on this diet (NS; $P = 0.09$). Thus, the db/db mice fed a MCD diet retained many of the features of the metabolic syndrome.

To determine whether these metabolic differences were associated with changes in body weight or food consumption, we treated separate cohorts of mice with the MCD diet for 4 weeks. **Table 3** shows the effect of the MCD diet on body weight and food consumption. All mice lost weight on the MCD diet, as expected; however, the weight loss was attenuated in the db/db mice compared with db/m mice: 13% versus 35%, respectively. The db/db MCD diet group remained significantly more obese than db/m mice on either diet. At the end of the dietary treatment, the db/db MCD group weighed 34.6 ± 2.2 g, compared with 21.3 ± 0.5 and 14.2 ± 0.3 g in db/m mice fed the control and MCD diet, respectively ($P < 0.05$). Considering the possibility that weight loss could have been associated with alterations in food consumption, we measured food intake over a 4 week period (Table 3). The MCD diet eliminated baseline hyperphagia in db/db mice; however, daily food consumption was not reduced compared with db/m mice on either diet.

Both subcutaneous and visceral fat compartments were differentially reduced by MCD feeding in db/m and db/db mice (**Fig. 1**). Subcutaneous fat was diminished significantly in both strains by the MCD diet: from 0.32 ± 0.04 to 0.13 ± 0.01 g in db/m mice ($P < 0.01$) and from 4.5 ± 0.15 to 3.0 ± 0.21 g in db/db mice ($P < 0.001$), corresponding to 60% and 34% reductions in db/m and db/db mice, respectively. In db/m mice, gonadal fat decreased from 0.52 ± 0.05 g in the control diet group to 0.05 ± 0.01 g in the MCD diet group, a 90% decrease ($P < 0.001$). In contrast, the decrease in gonadal fat in db/db mice receiving the MCD diet was less marked: from 4.1 ± 0.17 g for db/db mice fed a control diet to 3.1 ± 0.3 g in the MCD diet group ($P < 0.05$), a 23% reduction. Therefore, gonadal fat mass in db/db mice remained 60-fold higher than in db/m mice on the MCD diet.

To understand the potential mechanisms by which the MCD diet induces hepatic steatosis, we examined the effects of the MCD diet on hepatic genes involved in fatty acid synthesis, oxidation, uptake, and secretion. In db/db mice, gene expression of sterol-regulatory binding element binding protein 1c (SREBP-1c) was unaffected by MCD diet feeding; however, the SREBP-1c downstream targets SCD-1 and FAS were decreased significantly, from 0.9 ± 0.1 to 0.2 ± 0.1 and from 1.2 ± 0.2 to 0.5 ± 0.1, respectively, after 4 weeks of MCD feeding ($P < 0.05$). In

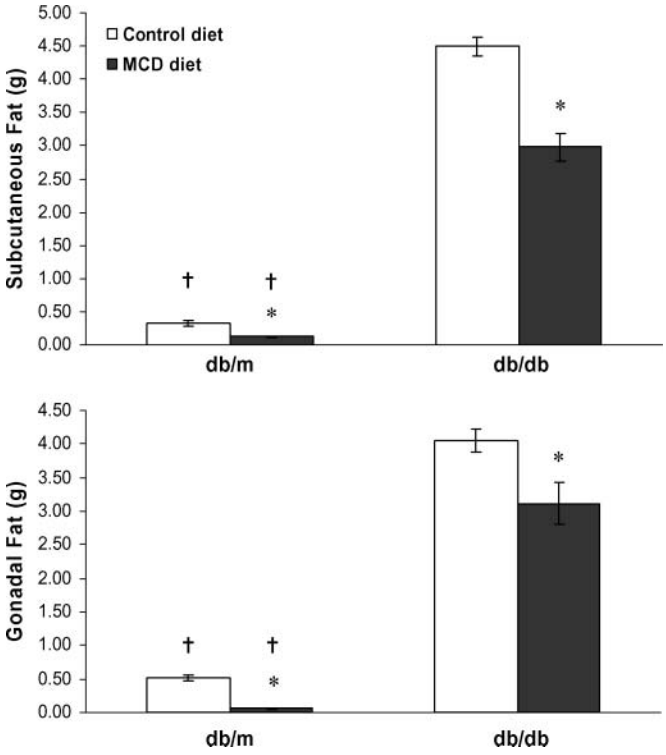

Fig. 1. Impact of the methionine choline-deficient (MCD) diet on the gonadal and subcutaneous fat compartments. Subcutaneous and gonadal fat were excised from db/m and db/db mice fed either a control diet or an MCD diet for 4 weeks. In both strains, the MCD diet led to significant reductions in both subcutaneous and gonadal fat depots. However, in db/db mice, gonadal fat loss was much less marked compared with db/m mice on the MCD diet. Values represent means of five mice ± SEM. * $P < 0.01$, effect of diet; † $P < 0.01$, effect of strain.

addition, gene expression of SREBP-1a was also decreased by the MCD diet in db/db mice (1.1 ± 0.2 and 0.6 ± 0.1; $P < 0.01$). The MCD diet significantly downregulated SREBP-1c and its downstream targets in db/m mice: 1.0 ± 0.1 and 0.6 ± 0.1 ($P = 0.02$), for control and MCD diet-fed mice, respectively (**Table 4**).

Serum β-hydroxybutyrate levels were compared between control diet-fed mice and MCD diet-fed mice as an overall measure of β-oxidation. The MCD diet did not significantly affect serum β-hydroxybutyrate levels: 0.2 ± 0.0 and 0.4 ± 0.2 mM for db/db mice and 0.3 ± 0.2 and 0.4 ± 0.2 mM for db/m mice on control and MCD diets, respectively. Activation of the peroxisome proliferator-activated receptor α (PPARα) pathway, a key regulator of β-oxidation in mice, can be a physiologic response to hepatic steatosis and increased fatty acid substrate. β-Oxidation gene expression, however, was not upregulated in the presence of hepatic steatosis induced by the MCD diet. Gene expression of the PPARα downstream target acyl-coenzyme A oxidase (AOX) was differentially affected in db/db and db/m mice by the MCD diet. In db/m mice, there was no significant change in AOX gene expression after the MCD diet (0.7 ± 0.1 vs. 0.9 ± 0.2). In db/db mice, AOX gene expression decreased in response to the MCD diet (1.0 ± 0.1 vs. 0.8 ± 0.1; $P < 0.05$). On a control diet, db/m mice had significantly lower AOX expression than db/db mice. Although the MCD diet appeared to increase carnitine palmitoyltransferase (CPT)-1 and -2, only CPT-2 increased in a statistically significant manner with the MCD diet in db/m mice. Fatty acid binding protein, however, was downregulated significantly by the MCD diet: 0.7 ± 0.0 versus 0.3 ± 0.0 and 0.8 ± 0.1 versus 0.6 ± 0.1 for db/db and db/m mice, respectively ($P < 0.001$) (Table 4).

TABLE 4. Real-time quantitative PCR of hepatic lipid genes in db/db and db/m mice treated with the MCD or the control diet for 4 weeks

	db/db Mice		db/m Mice	
Gene	Control Diet	MCD Diet	Control Diet	MCD Diet
Fatty acid synthesis				
SREBP-1a	1.1 ± 0.2[a,c]	0.6 ± 0.1	1.6 ± 0.2	1.4 ± 0.8
SREBP-1c	0.4 ± 0.1	0.6 ± 0.1	1.0 ± 0.1[d]	0.6 ± 0.1
SCD-1	0.9 ± 0.1[c]	0.2 ± 0.1	1.3 ± 0.4[d]	0.1 ± 0.0
FAS	1.2 ± 0.2[c]	0.5 ± 0.1	1.5 ± 0.4[d]	0.4 ± 0.0
β-oxidation				
AOX	1.0 ± 0.1[a,c]	0.8 ± 0.1	0.7 ± 0.1	0.9 ± 0.2
LCAD	0.6 ± 0.1	0.6 ± 0.1	0.5 ± 0.1	0.9 ± 0.1
L-FABP	0.7 ± 0.0[c]	0.3 ± 0.0[b]	0.8 ± 0.1[d]	0.6 ± 0.1
CPT-1	2.2 ± 0.9	5.0 ± 0.9	2.6 ± 1.0	3.5 ± 0.5
CPT-2	0.7 ± 0.1[a]	1.1 ± 0.2	0.9 ± 0.0[d]	1.2 ± 0.1
Fatty acid uptake				
FATP-1	0.7 ± 0.1[c]	1.4 ± 0.1	0.9 ± 0.3	1.3 ± 0.3
FATP-2	0.5 ± 0.0[a]	0.7 ± 0.1	0.8 ± 0.1[d]	0.7 ± 0.1
FATP-3	0.5 ± 0.1[c]	0.8 ± 0.1	0.8 ± 0.2	0.7 ± 0.1
FATP-4	1.2 ± 0.1[c]	2.6 ± 0.3	1.0 ± 0.2[d]	1.8 ± 0.2
FATP-5	0.3 ± 0.0	0.3 ± 0.0	0.6 ± 0.1	0.4 ± 0.0

Unpaired *t*-tests were used to compare the effect of the diet within a strain (n = 3–12 for each group). Values represent relative means ± SEM. For all, $P < 0.05$.

[a] db/db versus db/m mice on the control diet.
[b] db/db mice versus db/m mice on the MCD diet.
[c] db/db mice on the control versus the MCD diet.
[d] db/m mice on the control versus the MCD diet.

We subsequently identified the effects of the MCD diet on hepatic fatty acid uptake. First, we evaluated the hepatic expression of members of the fatty acid transport protein (FATP)/solute carrier family 27 genes. These transport proteins are thought to play an important role in hepatic fatty acid uptake, although the exact mechanisms by which they affect lipid uptake have not been clearly shown (22). In db/db mice, FATP-1, FATP-3, and FATP-4 were upregulated by 2-, 1.5-, and 2-fold, respectively, after 4 weeks of MCD diet feeding. FATP-2 and FATP-5 remained essentially unchanged (Table 4). The MCD diet also significantly increased the expression of FATP-4 in db/m mice: 1.0 ± 0.2 and 1.8 ± 0.2 ($P < 0.01$). To confirm that increased FATP gene expression correlated with a functional increase in hepatic fatty acid uptake, we measured [^{14}C]oleic acid uptake in MCD and control diet-fed mice after gavage with 2 μCi of [^{14}C]oleic acid (21). Both strains fed the MCD diet had dramatically increased fatty acid uptake. In db/m mice, uptake increased by 3-fold with the MCD diet ($P < 0.001$). Similarly, the MCD diet significantly increased hepatic [^{14}C]oleate uptake in db/db mice ($P < 0.01$) (**Fig. 2**). Thus, both gene expression and functional fatty acid uptake were increased by the MCD diet.

Total serum triglyceride levels in db/db mice decreased from 79 ± 3 to 56 ± 3 mg/dl in the MCD diet group ($P < 0.001$), and those in db/m mice decreased from 70 ± 4 to 45 ± 5 mg/dl ($P < 0.01$) (Table 2). Because impaired hepatic VLDL secretion can also lead to lipid accumulation (23), we subsequently examined the effects of the MCD diet on VLDL secretion. Triton WR-1339 inhibits lipoprotein lipase and blocks the breakdown of VLDL in the peripheral blood; thus, the increase in serum triglyceride levels measured after Triton WR-1339 injection in fasting mice is representative of hepatic VLDL secretion (24). After Triton WR-1339 administration, serum triglyceride levels increased in both db/db and db/m mice (**Fig. 3**). When triglyceride secretion rate was calculated in each strain, the MCD diet significantly reduced VLDL secretion in db/m mice ($P < 0.001$). In db/db

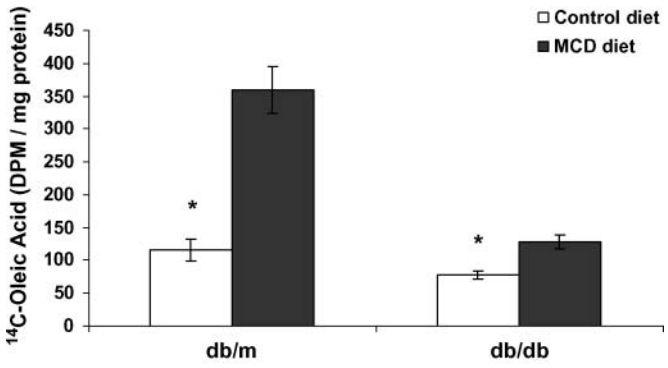

Fig. 2. Hepatic [^{14}C]oleic acid uptake at 4 h after oral gavage in db/m and db/db mice fed a control or MCD diet for 4 weeks. The MCD diet increased the hepatic uptake of [^{14}C]oleic acid by 3-fold in db/m mice and by nearly 2-fold in db/db mice. Values represent means of five mice ± SEM. * $P < 0.01$. Open bars, control diet; closed bars, MCD diet.

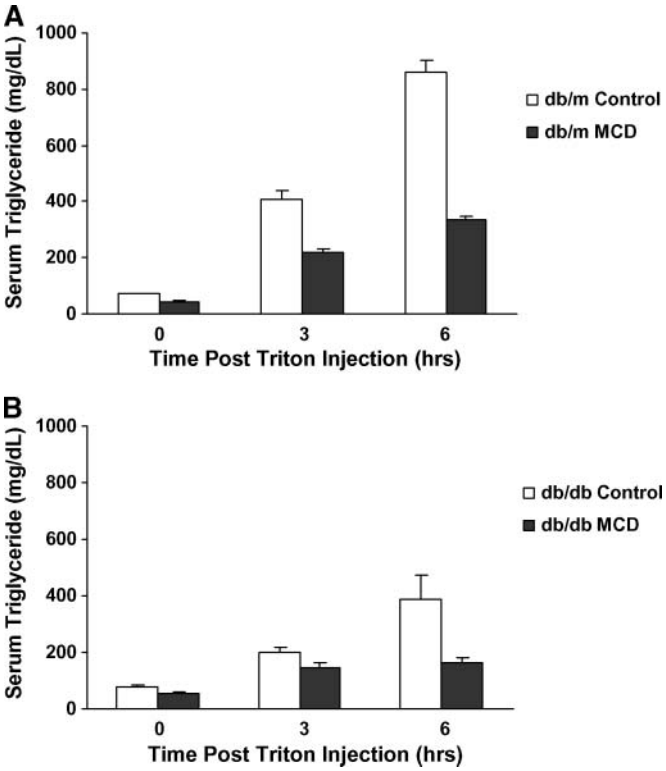

Fig. 3. Serum triglyceride levels after Triton WR-1339 injection in db/m and db/db mice fed a control or MCD diet for 4 weeks. Serum triglyceride secretion after Triton WR-1339 administration is blunted in MCD diet-fed db/m (A) and db/db (B) mice. Open and closed bars represent the control diet and the MCD diet, respectively. Values represent means of four mice ± SEM.

mice, VLDL secretion appeared to decrease, although this did not reach statistical significance ($P = 0.10$). db/m mice fed either a control or MCD diet had higher VLDL secretion rates than db/db mice on parallel diets ($P < 0.01$) (**Fig. 4**).

Western blot analysis of serum apoB-100 and apoB-48 before and after Triton WR-1339 treatment is shown in **Fig. 5**. At baseline (time 0), db/m mice fed a control diet had more apoB in the circulation than db/m mice fed the MCD diet, and this was composed almost entirely of apoB-100. In contrast, db/db mice on the control diet had decreased expression of both apoB-100 and apoB-48 compared with db/db mice on the MCD diet at baseline. Densitometric analysis using the integrated density function of ImageJ software was used to confirm qualitative findings (25).

When db/m mice on the control diet were compared with those fed the MCD diet, apoB-100 and apoB-48 protein secretion (defined by accumulation after Triton WR-1339 injection) was reduced in mice receiving the MCD diet. Thus, in db/m mice, both triglyceride and apoB secretion decreased with MCD diet feeding. In db/db mice fed the MCD diet, baseline expression of apoB-100 and apoB-48 was much higher compared with that in db/db mice on the control diet; however, apoB expression did not increase dramatically over time (Fig. 5). Serum lipoproteins were further analyzed in two

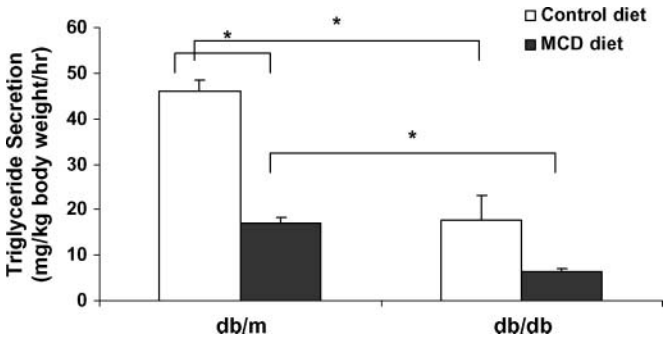

Fig. 4. Serum triglyceride secretion after Triton WR-1339 injection in db/m and db/db mice fed control and MCD diets for 4 weeks. Open and closed bars represent the control diet and the MCD diet, respectively. Values represent means of four mice ± SEM. * $P < 0.05$, significant difference between strains on a control diet, as determined by *t*-test.

additional cohorts (n = 4) with FPLC after 4 weeks of MCD diet administration. In db/db and db/m mice, the triglyceride content of the VLDL fraction was decreased by the MCD diet.

DISCUSSION

The mechanisms responsible for the development and progression of NASH in humans are complex and have not been fully delineated. Lipid initially accumulates in the liver through one or more of the following mechanisms: increased fatty acid uptake, increased triglyceride synthesis, decreased β-oxidation, or decreased hepatic export of triglycerides as VLDL. Insulin resistance has a well-accepted role in contributing to hepatic steatosis, and hepatic steatosis itself impairs insulin signaling (5, 6).

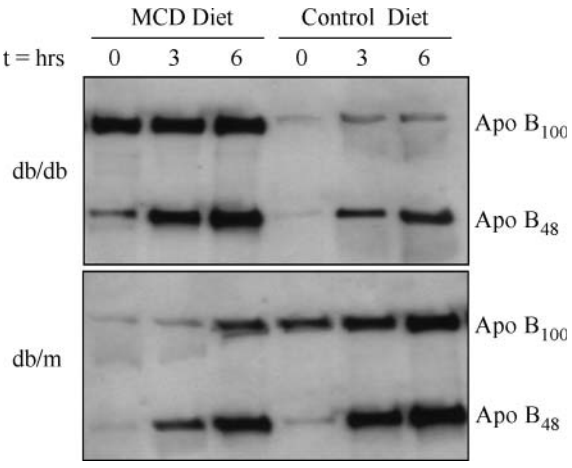

Fig. 5. Western blot of serum apolipoprotein B-100 (apoB-100) and apoB-48 in db/db and db/m mice fed either the MCD or control diet for 4 weeks. Time points represent hours after the administration of Triton WR-1339. In db/m mice, the MCD diet reduced apoB secretion. In db/db mice, baseline levels of apoB-100 and apoB-48 were increased in the MCD diet cohort. The rate of accumulation was more pronounced in apoB-48 than in apoB-100.

The lipogenic MCD diet induces severe liver disease that is histologically similar to human NASH. Here, we report the mechanisms by which the MCD diet leads to intrahepatic lipid accumulation in diabetic db/db mice and nondiabetic db/m mice. Although the MCD dietary model has known disparities with human NASH (12, 17), it has proven useful in exploring mechanisms of injury in steatohepatitis (26–30). Thus, it has become a well-accepted animal model for NASH. It is known that the MCD diet produces weight loss and improves peripheral insulin sensitivity (12). Here, we show that MCD diet-fed db/m mice lost 34.5% of their body weight after 4 weeks, similar to what we reported previously in FVB/NJ mice (8). This weight loss may be attributable in part to an increased metabolic rate in mice fed the MCD diet (17). The MCD diet did not have an effect on food intake in db/m mice; however, MCD diet-fed db/db mice were no longer hyperphagic. Because the MCD diet did not directly affect leptin levels, it is possible that the MCD diet could improve leptin signaling and thereby decrease the appetite in db/db mice that have defective leptin signaling at baseline.

The db/db mice did lose weight, but to a less dramatic degree: only 12.5% of their starting body weight after 4 weeks of the MCD diet. We show that despite weight loss and improved insulin sensitivity in the db/db mice after 4 weeks of the MCD diet, db/db mice remained more obese and insulin-resistant than the db/m mice on either diet. Therefore, improved insulin sensitivity in mice fed the MCD diet is overcome, in part, by using db/db mice in this model system. Importantly, recent data have shown that despite improved peripheral insulin sensitivity, hepatic insulin signaling is impaired in the MCD model, consistent with a state of hepatic insulin resistance (6, 26, 29). This is an important improvement over the MCD diet in nondiabetic lean mice, as human NASH typically occurs in the setting of obesity and insulin resistance. Furthermore, others have shown that the MCD diet may accentuate the liver injury seen in db/db mice and diabetic rats (11, 14, 31), and the markedly increased alanine aminotransferase levels in db/db mice fed the MCD diet shown here support this supposition.

Interestingly, although the MCD diet resulted in a significant reduction in both visceral and subcutaneous fat in db/m mice, the visceral fat compartment was relatively preserved in db/db mice after MCD feeding. Because visceral fat is more proinflammatory (32, 33) and was less affected by the MCD diet in db/db mice, this could partially explain why MCD diet-fed db/db mice develop more pronounced histological injury and a more proinflammatory profile (11, 14), despite weight loss induced by the diet.

We examined the gene expression of key lipid metabolic genes involved in triglyceride synthesis, fatty acid uptake, and oxidation and evaluated the effect of the MCD diet on the hepatic export of VLDL. These data demonstrate that the MCD diet promotes hepatic lipid accumulation by more than one mechanism. We found that at baseline, db/db mice had decreased expression of key genes of de novo lipogenesis. SREBP-1c gene expression was not increased in db/db mice fed a control diet, compared with db/m mice. These experiments were reproduced in several other cohorts using multiple housekeeping and SREBP-1c primers. Some of these differences may be explained by the nutritional content of both the MCD and MCD control diets (which differs from that of standard chow). Another possibility is that residual leptin short-form signaling in db/db mice plays a role (11). Thus, there are many potential explanations for the decreased expression of SREBP-1c downstream targets independent of SREBP-1c in db/db mice.

MCD feeding decreased FAS and SCD-1 gene expression, consistent with the hypermetabolic state recently described in MCD diet-fed mice (17). In this recent publication, downregulation of SCD-1 gene expression in MCD diet-fed mice correlated with the disappearance of SCD-1 protein from hepatic microsomes (17). In db/m mice, SREBP-1c was also decreased significantly by the MCD diet. Interestingly, the MCD diet did not downregulate SREBP-1c in db/db mice, despite the downregulation of its downstream targets. SREBP-1c is transcriptionally regulated by itself and the nuclear receptor liver X receptor. In addition, it is activated by insulin and glucose and reduced by leptin (34–37). Both FAS and SCD-1 can also be downregulated by other factors, such as leptin, independent of SREBP-1c and insulin (37, 38). Furthermore, if the MCD diet improves leptin signaling, leptin may more effectively downregulate the SREBP-1c pathway.

The expression of PPARα pathway genes (β-oxidation) was not markedly changed in db/db mice on the control diet at baseline or even in the presence of the more pronounced steatosis produced by the MCD diet. CPT-1, the key regulatory enzyme for fatty acid oxidation, increased in conjunction with CPT-2; however, the increase only reached statistical significance for CPT-2. Even if β-oxidation was

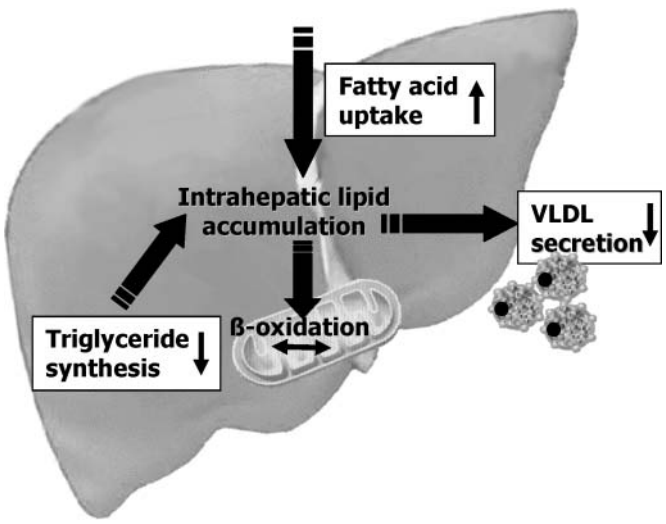

Fig. 6. Summary of the proposed mechanisms by which the MCD diet affects hepatic lipid metabolism. The MCD diet significantly increases fatty acid uptake and reduces VLDL secretion. Key genes involved in triglyceride synthesis are downregulated by MCD feeding.

increased to some degree by the MCD diet, it was not enough to offset the diet-induced increase in intrahepatic lipid. Weight loss and starvation can result in steatohepatitis and alterations of fatty acid oxidative and synthetic genes; however, when food intake was measured, we found that these changes were not explained by starvation. Furthermore, the lack of increase in serum β-hydroxybutyrate with MCD feeding does not support the notion that the MCD diet causes liver injury through starvation.

Previous rat studies using a choline-deficient (methionine-containing) diet suggested that hepatic steatosis may be attributable in part to impaired hepatic VLDL secretion (15). Our data show that the MCD diet reduced triglyceride and apoB secretion in db/m mice. In db/db mice, the MCD diet also decreased triglyceride secretion, but to a lesser degree. In contrast to db/m mice, apoB-100 and apoB-48 did not appear to be attenuated by the MCD diet in db/db mice. We speculate that this apparent discrepancy could be explained by a reduction in the triglyceride content of VLDL in the db/db MCD diet-fed group. In accordance with this speculation, FPLC of db/db mice fed the MCD diet illustrated a reduction in the triglyceride content of the VLDL fraction. If the MCD diet leads to decreased lipidation of VLDL particles, it is unlikely to be attributable to microsomal triglyceride transfer protein, whose gene expression was not changed by the MCD diet (data not shown). Baseline differences in serum apoB-100 and apoB-48 between db/db and db/m mice on the MCD diet suggest that db/db mice may have defective removal of apoB (39).

Hepatic fatty acid uptake is thought to occur by several mechanisms, including a transporter-mediated mechanism (40). The FATP family is thought to be an important regulator of fatty acid uptake (41). Of the known isoforms, FATP-5 and FATP-2 are strongly expressed in liver (21, 42), and FATP-1 and FATP-4 are present in liver in lower concentrations [22, 43. However, others have shown increased hepatic expression of FATP-1 and FATP-4 in a rat model of fatty liver (43). Furthermore, FATP-$5^{-/-}$ mice have increased expression of FATP-2 and FATP-3 (21). In the present study, gene expression of hepatic FATP-1, -3, and -4 was increased significantly by the MCD diet in db/db mice, suggesting that increased fatty acid uptake may be an important contributing factor in the development of hepatic steatosis induced by the MCD diet. Our data show that FATP-4 was also significantly upregulated in db/m mice after 4 weeks of MCD feeding. We further demonstrated that the MCD diet leads to a functional increase in hepatic fatty acid uptake of [^{14}C]oleate. In both strains, the MCD diet increased the hepatic uptake of [^{14}C]oleic acid, a novel mechanism of MCD diet-induced hepatic lipid accumulation. Thus, FATP-4 may be particularly important in mediating the enhanced hepatic oleic acid uptake in this experimental model. Humans with NAFLD have increased levels of serum free fatty acids compared with controls. In a recent study of patients with NAFLD, plasma fatty acids were shown to be the principal source of fat in hepatic triglyceride: 59% compared with only 25% from de novo lipogenesis or 13% from the diet (7).

Incorporating a diabetic rodent into the MCD model of steatohepatitis attenuates the apparent inconsistencies between the MCD dietary model and human NASH. In this model, peripheral insulin resistance is preserved to some degree and hepatic steatosis and injury are accentuated. Our data suggest that this may be attributable to the relative preservation of more metabolically active visceral fat in db/db mice compared with db/m mice fed an MCD diet. We demonstrate that increased hepatic uptake of [^{14}C]oleic acid is an important novel mechanism of MCD-induced hepatic steatosis (**Fig. 6**). Similarly, recent data in human NASH have shown that the predominant source of hepatic lipid is hepatic uptake in the setting of inappropriate peripheral lipolysis (7). Furthermore, we confirm the speculation that the MCD diet promotes lipid accumulation in the liver through the impairment of VLDL secretion. These data further validate the use of the MCD diet in diabetic rodents for the study of human NASH.

These studies were supported by Grant R01 DK-059580 (R.M.G.), by an American Gastroenterological Association Research Scholar Award, National Institutes of Health Grant K08 DK-066032 (M.E.R.), and by the Sidney and Bess Eisenberg Memorial Fund (J.B.).

REFERENCES

1. Skelly, M. M., P. D. James, and S. D. Ryder. 2001. Findings on liver biopsy to investigate abnormal liver function tests in the absence of diagnostic serology. *J. Hepatol.* **35:** 195–199.
2. Caldwell, S. H., D. H. Oelsner, J. C. Iezzoni, E. E. Hespenheide, E. H. Battle, and C. J. Driscoll. 1999. Cryptogenic cirrhosis: clinical characterization and risk factors for underlying disease. *Hepatology.* **29:** 664–669.
3. Sanjeevi, A., E. Lyden, B. Sunderman, R. Weseman, R. Ashwathnarayan, and S. Mukherjee. 2003. Outcomes of liver transplantation for cryptogenic cirrhosis: a single-center study of 71 patients. *Transplant. Proc.* **35:** 2977–2980.
4. Sanyal, A. J. 2005. Mechanisms of disease. Pathogenesis of nonalcoholic fatty liver disease. *Nat. Clin. Pract. Gastroenterol. Hepatol.* **2:** 46–53.
5. Sanyal, A. J., C. Campbell-Sargent, F. Mirshahi, W. B. Rizzo, M. J. Contos, R. K. Sterling, V. A. Luketic, M. L. Shiffman, and J. N. Clore. 2001. Nonalcoholic steatohepatitis: association of insulin resistance and mitochondrial abnormalities. *Gastroenterology.* **120:** 1183–1192.
6. Samuel, V. T., Z. X. Liu, X. Qu, B. D. Elder, S. Bilz, D. Befroy, A. J. Romanelli, and G. I. Shulman. 2004. Mechanism of hepatic insulin resistance in non-alcoholic fatty liver disease. *J. Biol. Chem.* **279:** 32345–32353.
7. Donnelly, K. L., C. I. Smith, S. J. Schwarzenberg, J. Jessurun, M. D. Boldt, and E. J. Parks. 2005. Sources of fatty acids stored in liver and secreted via lipoproteins in patients with nonalcoholic fatty liver disease. *J. Clin. Invest.* **115:** 1343–1351.
8. Leclercq, I. A., G. C. Farrell, R. Schriemer, and G. R. Robertson. 2002. Leptin is essential for the hepatic fibrogenic response to chronic liver injury. *J. Hepatol.* **37:** 206–213.
9. Aleffi, S., I. Petrai, C. Bertolani, M. Parola, S. Colombatto, E. Novo, F. Vizzutti, F. A. Anania, S. Milani, K. Rombouts, et al. 2005. Upregulation of proinflammatory and proangiogenic cytokines by leptin in human hepatic stellate cells. *Hepatology.* **42:** 1339–1348.
10. Sahai, A., P. Malladi, H. Melin-Aldana, R. M. Green, and P. F. Whitington. 2004. Upregulation of osteopontin expression is involved in the development of nonalcoholic steatohepatitis in a dietary murine model. *Am. J. Physiol. Gastrointest. Liver Physiol.* **287:** G264–G273.
11. Sahai, A., P. Malladi, X. Pan, R. Paul, H. Melin-Aldana, R. M. Green,

and P. F. Whitington. 2004. Obese and diabetic db/db mice develop marked liver fibrosis in a model of nonalcoholic steatohepatitis: role of short-form leptin receptors and osteopontin. *Am. J. Physiol. Gastrointest. Liver Physiol.* **287:** G1035–G1043.
12. Rinella, M. E., and R. M. Green. 2004. The methionine-choline deficient dietary model of steatohepatitis does not exhibit insulin resistance. *J. Hepatol.* **40:** 47–51.
13. Ip, E., G. Farrell, P. Hall, G. Robertson, and I. Leclercq. 2004. Administration of the potent PPARalpha agonist, Wy-14,643, reverses nutritional fibrosis and steatohepatitis in mice. *Hepatology.* **39:** 1286–1296.
14. Yamaguchi, K., L. Yang, S. McCall, J. Huang, X. X. Yu, S. K. Pandey, S. Bhanot, B. P. Monia, Y. X. Li, and A. M. Diehl. 2007. Inhibiting triglyceride synthesis improves hepatic steatosis but exacerbates liver damage and fibrosis in obese mice with nonalcoholic steatohepatitis. *Hepatology.* **45:** 1366–1374.
15. Yao, Z. M., and D. E. Vance. 1988. The active synthesis of phosphatidylcholine is required for very low density lipoprotein secretion from rat hepatocytes. *J. Biol. Chem.* **263:** 2998–3004.
16. Vance, J. E., and D. E. Vance. 1985. The role of phosphatidylcholine biosynthesis in the secretion of lipoproteins from hepatocytes. *Can. J. Biochem. Cell Biol.* **63:** 870–881.
17. Rizki, G., L. Arnaboldi, B. Gabrielli, J. Yan, G. S. Lee, R. K. Ng, S. M. Turner, T. M. Badger, R. E. Pitas, and J. J. Maher. 2006. Mice fed a lipogenic methionine-choline-deficient diet develop hypermetabolism coincident with hepatic suppression of SCD-1. *J. Lipid Res.* **47:** 2280–2290.
18. Reed, D. R., A. H. McDaniel, X. Li, M. G. Tordoff, and A. A. Bachmanov. 2006. Quantitative trait loci for individual adipose depot weights in C57BL/6ByJ × 129P3/J F2 mice. *Mamm. Genome.* **17:** 1065–1077.
19. Vanpatten, S., G. B. Karkanias, L. Rossetti, and D. E. Cohen. 2004. Intracerebroventricular leptin regulates hepatic cholesterol metabolism. *Biochem. J.* **379:** 229–233.
20. Fu, T., D. Mukhopadhyay, N. O. Davidson, and J. Borensztajn. 2004. The peroxisome proliferator-activated receptor alpha (PPARalpha) agonist ciprofibrate inhibits apolipoprotein B mRNA editing in low density lipoprotein receptor-deficient mice: effects on plasma lipoproteins and the development of atherosclerotic lesions. *J. Biol. Chem.* **279:** 28662–28669.
21. Doege, H., R. A. Baillie, A. M. Ortegon, B. Tsang, Q. Wu, S. Punreddy, D. Hirsch, N. Watson, R. E. Gimeno, and A. Stahl. 2006. Targeted deletion of FATP5 reveals multiple functions in liver metabolism: alterations in hepatic lipid homeostasis. *Gastroenterology.* **130:** 1245–1258.
22. Hirsch, D., A. Stahl, and H. F. Lodish. 1998. A family of fatty acid transporters conserved from mycobacterium to man. *Proc. Natl. Acad. Sci. USA.* **95:** 8625–8629.
23. Mensenkamp, A. R., M. J. Van Luyn, R. Havinga, B. Teusink, I. J. Waterman, C. J. Mann, B. M. Elzinga, H. J. Verkade, V. A. Zammit, L. M. Havekes, et al. 2004. The transport of triglycerides through the secretory pathway of hepatocytes is impaired in apolipoprotein E deficient mice. *J. Hepatol.* **40:** 599–606.
24. Tietge, U. J., A. Bakillah, C. Maugeais, K. Tsukamoto, M. Hussain, and D. J. Rader. 1999. Hepatic overexpression of microsomal triglyceride transfer protein (MTP) results in increased in vivo secretion of VLDL triglycerides and apolipoprotein B. *J. Lipid Res.* **40:** 2134–2139.
25. Abramoff, M. D., P. J. Magelhaes, and S. J. Ram. 2004. Image processing with ImageJ. *Biophotonics International.* **11:** 36–42.
26. Schattenberg, J. M., R. Singh, Y. Wang, J. H. Lefkowitch, R. M. Rigoli, P. E. Scherer, and M. J. Czaja. 2006. JNK1 but not JNK2 promotes the development of steatohepatitis in mice. *Hepatology.* **43:** 163–172.
27. Schattenberg, J. M., Y. Wang, R. Singh, R. M. Rigoli, and M. J. Czaja. 2005. Hepatocyte CYP2E1 overexpression and steatohepatitis lead to impaired hepatic insulin signaling. *J. Biol. Chem.* **280:** 9887–9894.
28. Leclercq, I. A., G. C. Farrell, C. Sempoux, A. dela Pena, and Y. Horsmans. 2004. Curcumin inhibits NF-kappaB activation and reduces the severity of experimental steatohepatitis in mice. *J. Hepatol.* **41:** 926–934.
29. Leclercq, I. A., V. A. Lebrun, P. Starkel, and Y. J. Horsmans. 2007. Intrahepatic insulin resistance in a murine model of steatohepatitis: effect of PPARgamma agonist pioglitazone. *Lab. Invest.* **87:** 56–65.
30. Dela Pena, A., I. Leclercq, J. Field, J. George, B. Jones, and G. Farrell. 2005. NF-kappaB activation, rather than TNF, mediates hepatic inflammation in a murine dietary model of steatohepatitis. *Gastroenterology.* **129:** 1663–1674.
31. Ota, T., T. Takamura, S. Kurita, N. Matsuzawa, Y. Kita, M. Uno, H. Akahori, H. Misu, M. Sakurai, Y. Zen, et al. 2007. Insulin resistance accelerates a dietary rat model of nonalcoholic steatohepatitis. *Gastroenterology.* **132:** 282–293.
32. Schaffler, A., J. Scholmerich, and C. Buchler. 2005. Mechanisms of disease. Adipocytokines and visceral adipose tissue—emerging role in nonalcoholic fatty liver disease. *Nat. Clin. Pract. Gastroenterol. Hepatol.* **2:** 273–280.
33. Lyon, C. J., R. E. Law, and W. A. Hsueh. 2003. Minireview. Adiposity, inflammation, and atherogenesis. *Endocrinology.* **144:** 2195–2200.
34. Lu, T. T., J. J. Repa, and D. J. Mangelsdorf. 2001. Orphan nuclear receptors as eLiXiRs and FiXeRs of sterol metabolism. *J. Biol. Chem.* **276:** 37735–37738.
35. Repa, J. J., G. Liang, J. Ou, Y. Bashmakov, J. M. Lobaccaro, I. Shimomura, B. Shan, M. S. Brown, J. L. Goldstein, and D. J. Mangelsdorf. 2000. Regulation of mouse sterol regulatory element-binding protein-1c gene (SREBP-1c) by oxysterol receptors, LXR-alpha and LXRbeta. *Genes Dev.* **14:** 2819–2830.
36. Horton, J. D., J. L. Goldstein, and M. S. Brown. 2002. SREBPs: activators of the complete program of cholesterol and fatty acid synthesis in the liver. *J. Clin. Invest.* **109:** 1125–1131.
37. Miyazaki, M., A. Dobrzyn, W. C. Man, K. Chu, H. Sampath, H. J. Kim, and J. M. Ntambi. 2004. Stearoyl-CoA desaturase 1 gene expression is necessary for fructose-mediated induction of lipogenic gene expression by sterol regulatory element-binding protein-1c-dependent and -independent mechanisms. *J. Biol. Chem.* **279:** 25164–25171.
38. Biddinger, S. B., M. Miyazaki, J. Boucher, J. M. Ntambi, and C. R. Kahn. 2006. Leptin suppresses stearoyl-CoA desaturase 1 by mechanisms independent of insulin and sterol regulatory element-binding protein-1c. *Diabetes.* **55:** 2032–2041.
39. Li, X., S. M. Grundy, and S. B. Patel. 1997. Obesity in db and ob animals leads to impaired hepatic very low density lipoprotein secretion and differential secretion of apolipoprotein B-48 and B-100. *J. Lipid Res.* **38:** 1277–1288.
40. Stremmel, W. 1989. Mechanism of hepatic fatty acid uptake. *J. Hepatol.* **9:** 374–382.
41. Coe, N. R., A. J. Smith, B. I. Frohnert, P. A. Watkins, and D. A. Bernlohr. 1999. The fatty acid transport protein (FATP1) is a very long chain acyl-CoA synthetase. *J. Biol. Chem.* **274:** 36300–36304.
42. Fitscher, B. A., C. M. Klaassen-Schluter, and W. Stremmel. 1995. Evidence for a hepatocyte membrane fatty acid transport protein using rat liver mRNA expression in *Xenopus laevis* oocytes. *Biochim. Biophys. Acta.* **1256:** 47–51.
43. Feng, A. J., and D. F. Chen. 2005. [The expression and the significance of L-FABP and FATP4 in the development of nonalcoholic fatty liver disease in rats.] *Zhonghua Gan Zang Bing Za Zhi.* **13:** 776–779.